Received: 1 August 2021 | Revised: 29 November 2021 | Accepted: 14 January 2022

DOI: 10.1002/dac.5114

RESEARCH ARTICLE

WILEY

High mobility enabled spatial and media-based modulated orthogonal frequency division multiplexing systems for beyond 5G wireless communications

Mehmet Başaran[1,2] | **Ertuğrul Başar**[3] | **Hakan Ali Çırpan**[4]

[1]Kartal R&D Center, Siemens San. Tic. A.S., Istanbul, Turkey

[2]Information and Communications Research Group, Informatics Institute, Istanbul Technical University, Istanbul, Turkey

[3]Department of Electrical and Electronics Engineering, Koc University, Istanbul, Turkey

[4]Department of Electronics and Communication Engineering, Istanbul Technical University, Istanbul, Turkey

Correspondence
Mehmet Başaran, Yakacik Caddesi No: 111, 34870 Kartal, Istanbul, Turkey.
Email: mehmetbasaran@itu.edu.tr

Summary

This paper introduces the concept of spatial and media-based modulated (SMBM) orthogonal frequency division multiplexing (OFDM) as a potential candidate for highly mobile next generation beyond 5G (B5G) wireless communications. The proposed SMBM-OFDM technique utilizes not only the transmit antenna and channel state indices but also OFDM subcarriers to improve the system performance under high mobility. In addition, this study sheds light on challenging fast time-varying channel estimation problem of MBM-based systems by using the linear minimum mean square error (LMMSE) approach due to its optimality to investigate the achievable system performance with the aid of basis expansion modeling. The minimum lower bound on the channel estimation error (Bayesian Cramer–Rao bound) is derived theoretically and shown to be attainable by the considered LMMSE estimator. Moreover, symbol detection performance is provided for different modulation types and higher mobile velocities. Simulation results demonstrate that SMBM-OFDM system under high mobility is able to provide around 12-dB performance gains in terms of both channel estimation and symbol detection error compared to conventional spatial modulation (SM)-OFDM systems without MBM. The presented framework is important due to addressing the high mobility support of SMBM-OFDM systems for B5G wireless communications in terms of achievable channel estimation and data detection performance.

KEYWORDS

basis expansion model, beyond 5G, channel estimation, high mobility, index modulation (IM), media-based modulation (MBM), orthogonal frequency division multiplexing (OFDM), spatial modulation (SM), time-varying channels

1 | INTRODUCTION

Next generation wireless communication systems are designed to provide ultra-reliability, low-latency, higher data rates, and better system performance even in highly mobile environments of beyond 5G (B5G) wireless networks.[1–5] In order to achieve these goals, massive multiple-input-multiple-output (MIMO), orthogonal frequency division

multiplexing (OFDM), and index modulation (IM) concepts are widely adopted to emerging transmission schemes owing to their high spectral and energy efficiencies.[5–8]

Under the IM family, spatial modulation (SM) is a promising solution for MIMO systems owing to its advantages such as less complex receiver hardware with a single radio frequency (RF) chain deployment, bandwidth efficiency, and interchannel-interference (ICI) elimination thanks to the transmission of additional SM bits to activate corresponding transmit antenna.[9–11] Recently, media-based modulation (MBM) has received great attention as a new modulation scheme where the transmission media (i.e., channel) is manipulated through the parasitic RF mirrors deployed at each of the transmit antennas.[12] Similar to the SM concept, additional information bits for MBM are conveyed to specify the ON/OFF status of RF mirrors resulting in modified antenna beam patterns.[13] According to its ON or OFF status, the reflector on the RF mirror allows the wave pass through or reflects the incoming wave, respectively, leading to a mirror activation pattern (MAP) that constitutes rich diversity in terms of channel environment. Due to the RF mirror placement, the number of virtual channels between the selected transmit and all receive antennas increases compared to the conventional single-input-multi-output (SIMO) communication systems. Owing to the modulation considered in fading channel, MBM becomes superior to conventional modulation formats.[12,13]

In recent years, mainly detection performance of IM-based systems is investigated in[14–24] rather than realistic channel estimation performance. In Shamasundar and Chockalingam,[14] multiuser MBM performance in a massive MIMO setting is investigated through compressed sensing (CS)-based algorithms. In Yildirim et al[15] and Bamisaye and Quazi,[16] the performance of quadrature channel modulation, which is the combination of quadrature SM and MBM, is studied from various aspects. In Basar and Altunbas,[17] space-time block code (STBC)-based channel modulation (i.e., MBM) is proposed. However, this work is further developed including SM concept in Yigit and Basar[18] by presenting the corresponding error probability. The system performance of MBM with generalized SM is investigated in Naresh and Chockalingam[19] and Oladoyinbo et al.[20] However, the authors extend their work on performance analysis considering the maximum likelihood (ML) detectors under imperfect channel state information (I-CSI) assumption in Naresh and Chockalingam.[21] In Shamasundar et al.,[22] MBM for the uplink massive MIMO systems is focused where CS-based detection algorithms are applied. A differential MBM is proposed in Naresh and Chockalingam[23] due to the differentially encoded consecutive MBM signal blocks. On the other hand, an analytical approach to obtain the error probability of OFDM-IM in fading channels is proposed in Ma et al.[24] Furthermore, a reference signal aided channel estimation approach is considered for time-invariant SMBM systems in Kabaci et al.[25] However, there are studies dealing with the high speed scenarios in vehicular communications by focusing on SM and IM implementation individually.[26,27]

SMBM and IM-based studies defined in previous works[11–27] analyze the system performance from the symbol detection point of view only assuming the perfect CSI (P-CSI) at the receiver. In addition, these studies mainly ignore the channel estimation and its effects to the system performance. However, pilot symbol-aided channel estimation technique is proposed and evaluated for OFDM-IM systems in Acar et al[28] assuming the time-invariant channels. On the other hand, pseudo-noise (PN) sequence-based channel estimation performance of TDS-OFDM systems is evaluated for block-wise and time-varying mobile channels in Basaran et al.[29,30] Similarly, PN sequence utilization in channel estimation can also be applied to OFDM-based underwater acoustic communication as well.[31,32] Also, only Naresh and Chockalingam[21] take into account errors on the channel estimation for only MBM systems by simply adding random noise to the actual channel fading coefficients to get rid of channel estimation.

In this study, we introduce the SMBM-OFDM concept to exploit not only the space and channel modulations but also OFDM to achieve a better error performance to be consistent with the ultra-reliable low-latency communications (URLLC) requirements in B5G under highly mobile wireless communications.[2] In addition, discrete Legendre polynomial basis expansion model (DLP-BEM)-based fast time-varying channel estimation approach is proposed for SMBM-OFDM system considering the high mobility support to be exploited in next generation communications. The channel estimation performance is determined by mean square error (MSE). In the proposed channel estimation approach, the PN sequences are inserted into the OFDM data as reference sequences to enable the detection of core OFDM signal embedded into the composite SMBM-OFDM transmit signal owing to the autocorrelation property of the PN sequences. Accordingly, higher mobile velocities, 240 and 480 km/h are considered as in traveling with cars and trains, respectively, in accordance with the specifications of URLLC for next generation communications considering high mobility support.[2] In addition, symbol detection performance is investigated in terms of symbol error rate (SER) for various modulation types and high mobile speeds (i.e., Doppler shifts). As a benchmark in comparison, the performance of conventional SM-OFDM systems is provided to show the superiority of the MBM integration to the existing SM-OFDM system in terms of system performance. To summarize, the main contributions of this paper are three-fold:

- SMBM-OFDM modulation technique is introduced to further enhance the system error performance in accordance with the URLLC specifications in next generation communications.
- Fast time-varying channel estimation concept for MBM-based systems, which has not been investigated yet, is proposed to support high mobility which is one of the inevitable requirements of next generation communication systems. Accordingly, the linear minimum mean square error (LMMSE) estimator is selected to demonstrate real system performance since the LMMSE is optimum thanks to the Gaussian distribution of both received signal (i.e., observations) and frequency-selective channel (i.e., parameter to be estimated).
- Bayesian Cramer–Rao bound (BCRB), which shows the achievable minimum error level for channel estimation, is derived. It is shown that LMMSE estimation is able to attain BCRB levels for the SMBM-OFDM system. The corresponding system performance is demonstrated such that significant error performance gains around 12 dB for both channel estimation and symbol detection are obtained compared to conventional SM-OFDM systems under same conditions to provide fair comparison.

The remaining of the paper is organized as follows. In Section 2, the system model is introduced. System performance investigation for SMBM-OFDM systems is analyzed in Section 3. The system performance measures are defined in Section 4. Simulation results are presented in Section 5. Finally, the study is concluded in Section 6.

Throughout the paper, the following notations are used. Small and bold letters (i.e., $\mathbf{a}$) denote vectors while capital and bold letters (i.e., $\mathbf{A}$) denote matrices. $(\cdot)^T, (\cdot)^*, (\cdot)^\dagger, \det|.|$ and $(\cdot)^{-1}$ represent transpose, complex conjugate, Hermitian conjugate, determinant and inverse of the matrix, respectively. $\mathbf{0}_{N\times M}$ and $\mathbf{I}_N$ stand for the all zero matrix and identity matrix with corresponding sizes, respectively. diag{.} and trace{.} indicate taking the diagonal elements of the matrix and the summation of the diagonal elements of the matrix, respectively. $\mathbb{R}^{A\times B}$ and $\mathbb{C}^A$ define the space for real and complex planes that contain of real and complex numbers for a matrix with size $A \times B$ and a column vector with length A, respectively.

2 | SMBM-OFDM SYSTEM

The system model of SMBM-OFDM is illustrated in Figure 1 where the main communication components of this system (i.e., the structures of the transmitter, channel, and receiver) are introduced in detail in this section.

2.1 | Transmitter model

The transmitter side comprises binary information source, M-ary modulator, inverse fast Fourier transform (IFFT) block, and reference sequence insertion for OFDM technique and an SMBM-OFDM mapper that specifies the active transmit antenna and RF mirror status to send the composite signal. The tasks and characteristics of each block can be explained in detail as follows. Information source generates η binary bits at each transmission period for the signal generation ($N \log_2 M$ bits), transmit antenna selection ($\log_2 N_t$ bits) and RF mirror activation (N_{rf} bits) according to OFDM, SM, and MBM techniques, respectively, where N, N_t, and N_{rf} denote the number of OFDM symbols, transmit antenna, and RF mirrors, respectively. Note that the spectral efficiency of SMBM-OFDM technique is defined by the total bits generated by the binary information source at the transmitter for each transmission interval (i.e., bits per channel use and bpcu) which is given by

$$\eta = N \log_2 M + \log_2 N_t + N_{rf} \text{ bpcu}. \tag{1}$$

The binary signal bits ($N \log_2 M$ bits) are converted to data signals with N multicarriers with respect to M-ary modulation format resulting in N data symbols. Then, these symbols are applied to IFFT module to obtain OFDM modulated symbols. In order to preserve the data signals from intersymbol-interference (ISI) effect that occurs due to multipath wireless channel environment and to make channel estimation possible for time-varying channels, reference sequences are interleaved into the OFDM data symbols by partitioning them. Different from conventional cyclic prefix (CP)-OFDM systems where CP is added in front of the OFDM data symbols to get rid of ISI, reference sequences are also inserted into the mid and last regions of OFDM data symbols to better capture the fast time-varying changes of the channel response in the channel estimation stage. Accordingly, the corresponding OFDM signal structure is illustrated

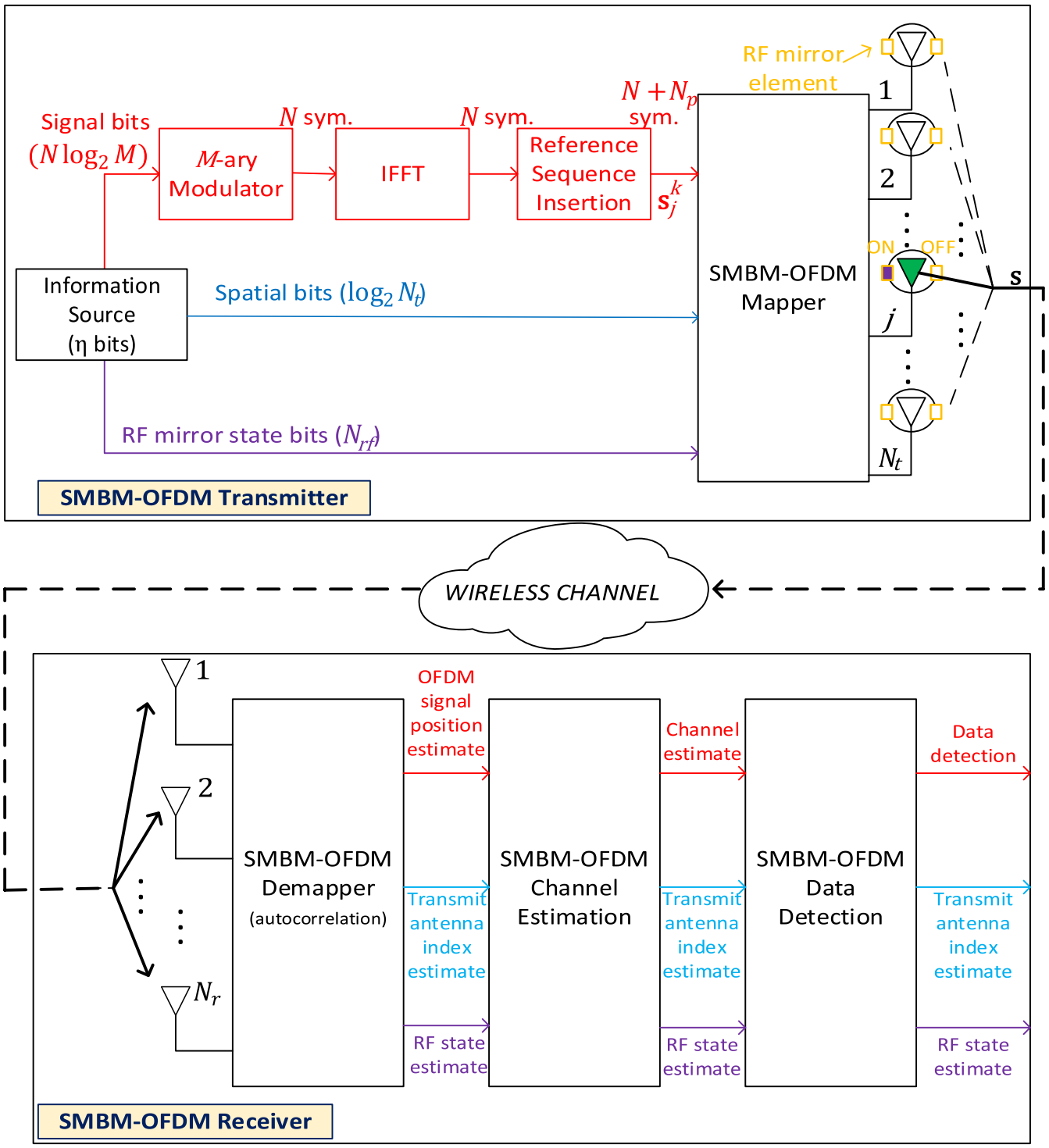

FIGURE 1 System model of SMBM-OFDM

in Figure 2 where first L-1 samples are ISI-corrupted and the remaining $N_{p_1}-L+1$ samples are in the ISI-free region, and thus, they can be utilized for channel estimation. Similarly, the mid and last reference sequences are used to catch the channel response better. The modulated OFDM signal has a length of $N_s=N+N_p$ where reference sequence length is $N_p=N_{p_1}+N_{p_2}+\ldots+N_{p_{\lambda+1}}$ while OFDM data length is $N=\sum_{i=1}^{\lambda}N_i$. On the other hand, energy efficiency can be considered when multiple users are communicating in the heterogeneous cellular network regions.[33–35]

Thanks to MBM, the SMBM-OFDM signal is composed of $N_{map}=2^{N_{rf}}$ blocks representing the channel state (i.e., constitutes the MAP) where every block is composed of N_t blocks in which the OFDM signal is placed according to

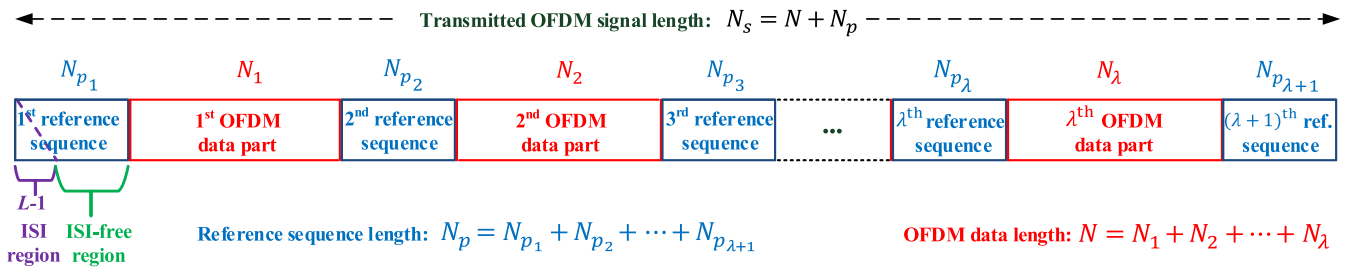

FIGURE 2 Transmitted OFDM signal structure

the specified transmit antenna in the context of SM. Therefore, the transmitted SMBM-OFDM signal can be represented in time domain as

$$\mathbf{s} = \left[\mathbf{s}_1^T | \mathbf{s}_2^T | ... | \mathbf{s}_{N_{map}}^T\right]^T \in \mathbb{C}^{N_s N_t N_{map}}. \tag{2}$$

Although symbol rate is slightly reduced due to the SM-MBM implementation to OFDM, its corresponding performance improves significantly as explained in detail in Section V.

Illustrative Toy Example: In order to illustrate the SMBM-OFDM signal transmission, a 4 × 4 MIMO system (with four transmit and four receive antennas, i.e., $N_t = N_r = 4$) is considered by assuming that the spatial bits ($\log_2 N_t$ bits) are generated as "01" and the RF mirror bits are generated as "10" among possible four channel states since the number of RF mirrors are deployed as $N_{rf} = 2$. Based on the corresponding SM and RF mirror bits, second transmit antenna and third channel state is determined by operating natural binary encoding (i.e., mapping bits as "00" to 1, "01" to 2, "10" to 3, and "11" to 4). Note that "10" RF bits denote the first RF mirror to be digitally ON position (marked with purple color at the jth transmit antenna marked with green color) while the second RF mirror to be stayed digitally OFF position. This RF mirror status corresponds to the one channel realization among possible $N_{map} = 2^{N_{rf}}$ channel realizations. Accordingly, SMBM-OFDM mapper block places the $\mathbf{s}_{j=2}^{k=3}$ OFDM signal to the location that takes place in the second OFDM data block inside the third channel state symbol block. The corresponding transmitted signal is created as

$$\mathbf{s} = \Big[\overbrace{\mathbf{0}_{N_s N_t}^T}^{\text{1st channel state symbols}} |\mathbf{0}_{N_s N_t}^T| \quad \overbrace{\mathbf{0}_{N_s}^T \underbrace{\mathbf{s}_2^{3T}}_{\text{2nd transmit antenna activation (i.e.,SM)}} \mathbf{0}_{N_s}^T \mathbf{0}_{N_s}^T}^{\text{3rd channel state symbols (i.e.,MBM)}} \quad |\mathbf{0}_{N_s N_t}^T\Big]^T, \tag{3}$$

where the core OFDM signal is embedded into the corresponding location specified by the SM and RF mirror bits.

The core data signal that conveys the nonzero OFDM symbols can be expressed as

$$\mathbf{s}_j^k = \left[\mathbf{p}_1^T, \mathbf{d}_1^T, \mathbf{p}_2^T, \mathbf{d}_2^T, ..., \mathbf{p}_\lambda^T, \mathbf{d}_\lambda^T, \mathbf{p}_{\lambda+1}^T\right]^T \in \mathbb{C}^{N_s}, \tag{4}$$

where $j \in \{1, 2, \dots, N_t\}$, $k \in \{1, 2, \dots, N_{map}\}$, and $\lambda + 1$ represents the number of reference sequences deployed while

$$\mathbf{p}_q = \left[p_q[0], p_q[1], ..., p_q[N_{p_q} - 1]\right]^T \in \mathbb{C}^{N_{p_q}} \tag{5}$$

defines the utilized reference sequences. The reference signal waveform is selected based on the Chu sequence for $q = 1, 2, ..., \lambda + 1$ due to its constant amplitude and zero autocorrelation properties which make it quite suitable to synchronize the OFDM signal in time-domain and accordingly allows the time-domain channel estimation of an OFDM signal.[30] The reference sequence waveform is expressed in Chu[36] as

$$p_q[n] = \begin{cases} \exp\left(-j\dfrac{\pi a n^2}{N_{p_q}}\right), & N_{p_q} \text{ even}, \\ \exp\left(-j\dfrac{\pi a n(n+1)}{N_{p_q}}\right), & N_{p_q} \text{ odd}, \end{cases} \tag{6}$$

where a is an integer and should be selected that the coprimeness with the sequence length, N_{p_q}, holds. The number of reference sequences are decided by taking into account the polynomial degree, λ, which is used to model the fast time-varying channel, and it will be explained in the next subsection in detail while explaining the BEM. On the other hand, OFDM data signals can be expressed as

$$\begin{aligned} \mathbf{d}_1 &= [d[0], d[1], ..., d[N_1 - 1]]^T \in \mathbb{C}^{N_1} \\ \mathbf{d}_2 &= [d[N_1], d[N_1 + 1], ..., d[N_1 + N_2 - 1]]^T \in \mathbb{C}^{N_2} \\ \mathbf{d}_i &= [d[N_1 + N_2 + ... + N_{i-1}], d[N_1 + N_2 + ... + N_{i-1} + 1], \\ &\quad ..., d[N_1 + N_2 + ... + N_i - 1]]^T \in \mathbb{C}^{N_i}, \end{aligned} \tag{7}$$

where $i = 3, 4, ..., \lambda$. The corresponding OFDM symbols in time domain is calculated as

$$d[n] = \frac{1}{N} \sum_{k=-N/2}^{N/2-1} b[k] e^{j2\pi n \frac{k}{N}} (u[n] - u[n-N]), \tag{8}$$

for $0 \leq n < N$, where n, k, and $u[n]$ stand for the indices in discrete-time and frequency domains and unit step function, respectively. $\mathbf{b} = [b[0], b[1], ..., b[N-1]]^T$ is the vector containing modulated OFDM data symbols corresponding to all subcarriers in the frequency domain. Accordingly, the SMBM-OFDM transmit signal is sent to the receiver through the channel over one RF chain.

2.2 | Channel model

Due to highly mobile communication environment, the multipath channel response to the each transmitted symbol varies over time. Therefore, the channel model can be expressed in vector form as

$$\mathbf{h} = [\mathbf{h}_1^T, \mathbf{h}_2^T, ..., \mathbf{h}_{N_r}^T]^T \in \mathbb{C}^{LN_sN_tN_rN_{map}}, \tag{9}$$

where N_r denotes the number of receive antennas. The channel between the transmit antennas and ith receiver is represented in terms of multipath components for $\ell = 0, 1, ..., L-1$ by

$$\mathbf{h}_i = \left[\mathbf{h}_i^{0^T}, \mathbf{h}_i^{1^T}, ..., \mathbf{h}_i^{L-1^T}\right]^T \in \mathbb{C}^{LN_sN_tN_{map}}, \tag{10}$$

with $i = 1, 2, ..., N_r$ being the receive antenna index. This channel can be further expressed as a combination of channel fade coefficients according to the channel state index, $k = 1, 2, ..., N_{map}$, as

$$\mathbf{h}_i^{\ell} = \left[\mathbf{h}_i^{\ell,1^T}, \mathbf{h}_i^{\ell,2^T}, ..., \mathbf{h}_i^{\ell,N_{map}{}^T}\right]^T \in \mathbb{C}^{N_sN_tN_{map}}. \tag{11}$$

Considering the specified transmit antenna index, the channel between ith receive and jth transmit antenna at the kth channel state can be written as

$$\mathbf{h}_i^{\ell,k} = \left[\mathbf{h}_{i,1}^{\ell,k^T}, \mathbf{h}_{i,2}^{\ell,k^T}, ..., \mathbf{h}_{i,N_t}^{\ell,k^T}\right]^T \in \mathbb{C}^{N_s N_t}. \tag{12}$$

The each corresponding channel in MBM is assumed to have wide sense stationary uncorrelated scattering (WSSUS) time-varying fading coefficients and can be described for each channel paths, $\ell = 0, 1, ..., L-1$, as

$$\mathbf{h}_{i,j}^{\ell,k} = \left[h_{i,j}^k[0,\ell], h_{i,j}^k[1,\ell], ..., h_{i,j}^k[N_s-1,\ell]\right]^T \in \mathbb{C}^{N_s}, \tag{13}$$

where $h_{i,j}^k[n,\ell]$ represents WSSUS Rayleigh fading channel coefficient.

Since the time-varying MBM channel contains more coefficients than the observations, the multipath channel can be represented by suitably building BEM thanks to the inherently banded structure of channel matrix.[37]

Accordingly, fast time-varying channel fading coefficients can be approximated by DLP-BEM in terms of the weighted sums of the orthogonal basis functions, $\{\psi_q(n)\}$, and basis coefficients (i.e., reduced sized channel coefficients), $\{c_{i,j}^k[q,\ell]\}$, using less number of basis functions, λ (i.e., the DLP degree) as

$$\tilde{h}_{i,j}^k[n,\ell] = \sum_{q=0}^{\lambda-1} c_{i,j}^k[q,\ell]\psi_q(n), \tag{14}$$

where $\tilde{h}_{i,j}^k[n,\ell]$ expresses the equivalent version of real channel. Note that considering the polynomial degree, we utilize $\lambda+1$ pilot sequences in the core OFDM signal in (4) both to express the equivalent channel model suitably with low modeling error,[38] and thus, to estimate the channel.

Utilizing the orthogonality property of basis functions and applying inverse transform, the equivalent channel and corresponding channel basis coefficients can be constructed in matrix-vector form as

$$\tilde{\mathbf{h}}_{i,j}^{\ell,k} = \mathbf{\Psi}_{i,j}^k \mathbf{c}_{i,j}^{\ell,k} \tag{15}$$

$$\text{and } \mathbf{c}_{i,j}^{\ell,k} = \mathbf{\Psi}_{i,j}^{k^T} \mathbf{h}_{i,j}^{\ell,k}, \tag{16}$$

respectively, where

$$\tilde{\mathbf{h}}_{i,j}^{\ell,k} = \left[\tilde{h}_{i,j}^k[0,\ell], \tilde{h}_{i,j}^k[1,\ell], ..., \tilde{h}_{i,j}^k[N_s-1,\ell]\right]^T \in \mathbb{C}^{N_s}, \tag{17}$$

$$\mathbf{c}_{i,j}^{\ell,k} = \left[c_{i,j}^k[0,\ell], c_{i,j}^k[1,\ell], ..., c_{i,j}^k[\lambda-1,\ell]\right]^T \in \mathbb{C}^{\lambda}, \tag{18}$$

and the matrix $\mathbf{\Psi}_{i,j}^k$ can be expressed over orthogonal basis functions as

$$\mathbf{\Psi}_{i,j}^k = \left[\boldsymbol{\psi}_{i,j}^k[0], \boldsymbol{\psi}_{i,j}^k[1], ..., \boldsymbol{\psi}_{i,j}^k[N_s-1]\right]^T \in \mathbb{R}^{N_s \times \lambda}, \tag{19}$$

with

$$\boldsymbol{\psi}_{i,j}^k[n] = \left[\psi_{i,j}^{k,0}(n), \psi_{i,j}^{k,1}(n), ..., \psi_{i,j}^{k,\lambda-1}(n)\right]^T, \tag{20}$$

where BEM polynomials, $\psi_{i,j}^{k,q}(n)$, can be generated by Gram–Schmidt method as detailed in Basaran et al.[30]

2.3 | Receiver model

The received SMBM-OFDM signal transmitted from jth antenna to the ith receive antenna can be expressed as

$$r_i(n) = \sum_{\ell=0}^{L-1} h_{i,j}[n,\ell]s[n-\ell] + w_i(n), \tag{21}$$

where $n = 0,1,...,N_sN_tN_{map}-1, j = 1,2,...,N_t, i = 1,2,...,N_r$, and $w_i(\cdot)$ denotes zero mean complex AWGN with variance N_0. As the multipath structure of the channel leads to the ISI on the symbols $s[-L+1], s[-L+2], \dots, s[-1]$ for the initial part of the transmit signal, ISI corrupted observation samples can be removed at the receiver as in CP discarding in conventional OFDM systems. Accordingly, the ISI-free observations can be defined as

$$\begin{aligned} y_i(n) &= r_i(n+L-1) \\ &= \sum_{\ell=0}^{L-1} h_{i,j}[n+L-1,\ell]s[n+L-1-\ell] + w_i(n+L-1) \end{aligned} \tag{22}$$

for $n = 0,1,...,N_sN_tN_{map}-L$. In the vector form, the signal at the ith receive antenna can be written as

$$\mathbf{y}_i = \sum_{\ell=0}^{L-1} \mathrm{diag}(\mathbf{s}_\ell)\mathbf{h}_{i,j}^{\ell} + \mathbf{w}_i \ \in \mathbb{C}^{N_\ell}, \tag{23}$$

where $N_\ell = N_sN_tN_{map} - L + 1$ denotes the ISI-free SMBM-OFDM observation length and

$$\mathbf{y}_i = \left[y_i[0], y_i[1], ..., y_i[N_sN_tN_{map}-L]\right]^T \in \mathbb{C}^{N_\ell}, \tag{24}$$

$$\mathbf{w}_i = \left[w_i[L-1], w_i[L], ..., w_i[N_sN_tN_{map}-1]\right]^T \in \mathbb{C}^{N_\ell}, \tag{25}$$

$$\mathbf{h}_{i,j}^{\ell} = \left[h_{i,j}[L-1,\ell], h_{i,j}[L,\ell], ..., h_{i,j}[N_sN_tN_{map}-1,\ell]\right]^T \in \mathbb{C}^{N_\ell}. \tag{26}$$

The transmit signal vector corresponding to the ℓth path can be written as

$$\mathbf{s}_0 = \left[s[L-1], s[L], ..., s[N_sN_tN_{map}-1]\right]^T \in \mathbb{C}^{N_\ell}, \ell = 0 \tag{27}$$

$$\begin{aligned} \mathbf{s}_\ell &= [s[L-1-\ell], s[L-\ell], \\ &\quad ..., s[N_sN_tN_{map}-1-\ell]\big]^T \in \mathbb{C}^{N_\ell}, 1 \le \ell \le L-1, \end{aligned} \tag{28}$$

where $\mathbf{s}_0$ and $\mathbf{s}_\ell$ defines the ISI removed transmit symbols and the shifted versions of the ISI-free signal stemming from the multipath channel, respectively.

Due to removing ISI contaminated components on the observations, and therefore, leading to redundant corresponding channel coefficients, the time-varying complete channel vector of the ℓth path in (13) can be redefined as

$$\mathbf{h}_{i,j}^{\ell,k} = \left[h_{i,j}^{k}[L-1,\ell], h_{i,j}^{k}[L,\ell], ..., h_{i,j}^{k}[N_s-1,\ell]\right]^T \in \mathbb{C}^{N_f}, \tag{29}$$

where $N_f = N_s - L + 1$ denotes the ISI-free core OFDM signal length.

In order to build received signal in linear form, the channel vector and the transmission matrix are defined suitably as

$$\mathbf{h}_i = \left[\mathbf{h}_i^{0^T}, \mathbf{h}_i^{1^T}, ..., \mathbf{h}_i^{L-1^T}\right]^T \in \mathbb{C}^{LN_\ell}, \tag{30}$$

$$\mathbf{S} \triangleq [\mathbf{S}_0, \mathbf{S}_1, ..., \mathbf{S}_{L-1}] \in \mathbb{C}^{N_\ell \times LN_\ell}, \tag{31}$$

where

$$\mathbf{S}_\ell = \text{diag}(\mathbf{s}_\ell). \tag{32}$$

Then, the signal at the ith receive antenna can be properly determined as

$$\mathbf{y}_i = \mathbf{S}\mathbf{h}_i + \mathbf{w}_i. \tag{33}$$

By using the alternative way over the channel matrix regarding the ith receive antenna, $\mathbf{H}_i$, the received signal can be defined as

$$\mathbf{y}_i = \mathbf{H}_i\mathbf{s} + \mathbf{w}_i, \tag{34}$$

where

$$\begin{aligned}\mathbf{H}_i &= \sum_{\ell=0}^{L-1} \text{cshift}\left([\mathbf{0}_{N_\ell \times (L-1)}, \text{diag}(\mathbf{h}_i^\ell)], -\ell\right) \\ &\in \mathbb{C}^{N_\ell \times N_s N_t N_{map}},\end{aligned} \tag{35}$$

with $\text{cshift}(\mathbf{L}, -\ell)$ representing column-wise ℓ-step circular counter clockwise shift of $\mathbf{L}$ matrix.

By using (15), the equivalent time-varying channel in MBM can be defined through basis functions and basis fading coefficients as

$$\mathbf{h}_i = \mathbf{\Phi}_i\mathbf{c}_i, \tag{36}$$

where

$$\mathbf{c}_i = \left[\mathbf{c}_i^{0^T}, \mathbf{c}_i^{1^T}, ..., \mathbf{c}_i^{L-1^T}\right]^T \in \mathbb{C}^{L\lambda N_t N_{map}}, \tag{37}$$

$$\mathbf{\Phi}_i = \mathbf{I}_L \otimes \mathbf{\Psi}_i \in \mathbb{C}^{LN_\ell \times L\lambda N_t N_{map}}, \tag{38}$$

with $\otimes$ denoting Kronecker product and to express the received signal in linear form $\mathbf{\Psi}_i$ is extended from (19) considering the ISI removal as

$$\mathbf{\Psi}_i = \left[\boldsymbol{\psi}_i[L-1], \boldsymbol{\psi}_i[L], ..., \boldsymbol{\psi}_i[N_s N_t N_{map} - 1]\right]^T \in \mathbb{R}^{N_\ell \times \lambda N_t N_{map}}. \tag{39}$$

Consequently, the received signal can be defined over BEM equivalent of the MBM channel as

$$\mathbf{y}_i = \mathbf{S}\mathbf{\Phi}_i\mathbf{c}_i + \mathbf{w}_i = \mathbf{Q}_i\mathbf{c}_i + \mathbf{w}_i, \tag{40}$$

where $\mathbf{Q}_i \triangleq \mathbf{S}\mathbf{\Phi}_i$ can be further named as observation matrix.

3 | CHANNEL ESTIMATION AND DATA DETECTION

In this section, channel estimation is explained first. Then, symbol detection is introduced for SMBM-OFDM systems operating under fast time-varying channels (i.e., highly mobile communication environments).

3.1 | Channel estimation for SMBM-OFDM systems

First, the location of core signal located in the sparse transmit signal which is modulated jointly by SM and MBM for transmit antenna index and channel state, respectively, should be determined. Owing to the autocorrelation property of the PN sequences, the received signal can be projected onto the signal itself leading to the detection of core transmit OFDM signal location as

$$\hat{\tau} = arg\ \underset{\tau}{max}\left\{\left|\sum_{n=0}^{N_\ell-1} y_i(n+\tau)y_i^*(n+\tau+N_\ell)\right|\right\}, \tag{41}$$

where $\hat{\tau}$ contains information belonging to the estimation of active transmit antenna index and channel state index, $\hat{j}$ and $\hat{k}$, respectively. Following the estimation of active transmit antenna and channel state indices (i.e., j and k are known), the equivalent reduced-sized received signal waveform can be expressed owing to sparsity as

$$\mathbf{y}_{i_{eq}} = \mathbf{S}_{eq}\mathbf{h}_{i,j}^{k} + \mathbf{w}_{i_{eq}}, \tag{42}$$

where

$$\mathbf{S}_{eq} = [\mathbf{S}_{0_{eq}}, \mathbf{S}_{1_{eq}}, ..., \mathbf{S}_{L-1_{eq}}] \in \mathbb{C}^{N_f \times LN_f}, \tag{43}$$

$$\mathbf{h}_{i,j}^{k} = \left[\mathbf{h}_{i,j}^{0,k^T}, \mathbf{h}_{i,j}^{1,k^T}, ..., \mathbf{h}_{i,j}^{L-1,k^T}\right]^T \in \mathbb{C}^{LN_f}, \tag{44}$$

and

$$\begin{aligned}\mathbf{w}_{i_{eq}} &= [w_i[(k-1)N_sN_t + (j-1)N_s + L - 1], w_i[(k-1)N_sN_t \\ &\quad + (j-1)N_s + L], ..., w_i[(k-1)N_sN_t + jN_s - 1]]^T \in \mathbb{C}^{N_f},\end{aligned} \tag{45}$$

with $\mathbf{S}_{\ell_{eq}} = \mathrm{diag}(\mathbf{s}_{\ell_{eq}}) \in \mathbb{C}^{N_f}$ consisting of the meaningful OFDM modulated transmit symbols.

Thanks to the known reference sequences deployed inside the OFDM modulated transmit symbols, unknown channel basis coefficients can be estimated by taking the ISI-free region into account on the reference sequence transmission. Note that reference signal length is not affected by the SM and MBM (i.e., transmit antenna selection and RF mirror deployment) and only proportional to OFDM subcarrier length to represent the fast time-varying channel polynomial suitably. In theoretical-sense, the ISI-free region equivalence in the observation matrix can be extracted to create a reduced sized observations to be used in the estimation of channel basis coefficients. Accordingly, the reduced-sized ISI-free received signal observed on the pilot symbols can be extracted from (42) to be defined in linear form by selecting time instants suitably as

$$\mathbf{z}_i = \mathbf{P}\mathbf{h}_{i,j}^{k} + \mathbf{n}_i = \mathbf{\Gamma}_i\mathbf{c}_{i,j}^{k} + \mathbf{n}_i \in \mathbb{C}^D, \tag{46}$$

where $\mathbf{n}_i$ can be viewed as a corresponding noise subvector, D represents the summation of ISI-free reference sequence region lengths whose the components in related region are used for channel estimation and can be expressed as

$$D=\sum_{q=1}^{\lambda+1}N_{p_q}-L+1, \tag{47}$$

and

$$\mathbf{c}_{i,j}^{k}=\left[\mathbf{c}_{i,j}^{0,k^T},\mathbf{c}_{i,j}^{1,k^T},...,\mathbf{c}_{i,j}^{L-1,k^T}\right]^T\in\mathbb{C}^{L\lambda} \tag{48}$$

represent the basis coefficients corresponding to core transmit OFDM signal samples.

The corresponding observation submatrix, $\boldsymbol{\Gamma}_i$, is defined as

$$\boldsymbol{\Gamma}_i=\mathbf{P}\boldsymbol{\Phi}_{i,j}^{k}, \tag{49}$$

where $\boldsymbol{\Phi}_{i,j}^{k}$ denotes the submatrix constructed according to the active transmit antenna and channel status similar to (38) and $\mathbf{P}$ represents the transmission submatrix which can be defined as

$$\mathbf{P}\triangleq[\mathbf{P}_1,\mathbf{P}_2,...,\mathbf{P}_{\lambda+1}]\in\mathbb{C}^{D\times N_fL}. \tag{50}$$

The inner components of transmission submatrix consist of pilot symbols and can be expressed as

$$\mathbf{P}_q=[\mathrm{diag}(\mathbf{p}_q),\mathbf{0}_{(N_{p_q}-L+1)\times(N_s-N_{p_q})}]\in\mathbb{C}^{D\times N_f} \tag{51}$$

where $\mathbf{p}_q$ is defined in (5). To illustrate more clearly, the useful observations suitable for channel estimation for the each receive antenna (i.e., $i=1,2,...,N_r$) are collected from the combination of multiple ISI-free regions and can be expressed in terms of the ISI-free region combinations as

$$\mathbf{z}_i=\left[\mathbf{z}_0^T,\mathbf{z}_1^T,...,\mathbf{z}_\lambda^T\right]^T, \tag{52}$$

where

$$\mathbf{z}_0=\left[y_{i_{eq}}[0],y_{i_{eq}}[1],...,y_{i_{eq}}[N_{p_1}-L]\right]^T, \tag{53}$$

while

$$\begin{aligned}\mathbf{z}_q=\Big[&y_{i_{eq}}[N_{p_1}+N_{p_2}+...+N_{p_q}+N_1+N_2+...+N_q],\\&y_{i_{eq}}[N_{p_1}+N_{p_2}+...+N_{p_q}+N_1+N_2+...+N_q+1],...,\\&y_{i_{eq}}[N_{p_1}+N_{p_2}+...+N_{p_{q+1}}+N_1+N_2+...+N_q-L]\Big]^T,\end{aligned} \tag{54}$$

for $1\leq q\leq\lambda$.

Following the considered assumptions on the transmit signal, channel, and observation signal, LMMSE estimate of the channel basis coefficients are determined for the linear system model given in (46) by the following formula:

$$\hat{\mathbf{c}}_{i,j}^{k}=\left(\boldsymbol{\Gamma}_i^{\dagger}\boldsymbol{\Gamma}_i+N_0\mathbf{R}_{\mathbf{c}_{i,j}^{k}}^{-1}\right)^{-1}\boldsymbol{\Gamma}_i^{\dagger}\mathbf{z}_i, \tag{55}$$

where $\mathbf{R}_{\mathbf{c}_{i,j}^{k}}$ represents autocorrelation matrix of basis coefficients belonging to the channel with respect to the ith receive antenna in which the autocorrelation matrix can be calculated as

$$\mathbf{R}_{\mathbf{c}_{i,j}^k} = \mathbb{E}\left[\mathbf{c}_{i,j}^k \mathbf{c}_{i,j}^{k\,\dagger}\right] = \mathbf{\Phi}_{i,j}^{k^\dagger} \mathbf{R}_{\mathbf{h}_{i,j}^k} \mathbf{\Phi}_{i,j}^k. \tag{56}$$

Here, $\mathbf{R}_{\mathbf{h}_{i,j}^k} = \mathbb{E}\left[\mathbf{h}_{i,j}^k \mathbf{h}_{i,j}^{k\,\dagger}\right]$ expresses the autocorrelation matrix of the channel coefficients. It can be written easily as

$$\mathbf{R}_{\mathbf{h}_{i,j}^k} = \text{diag}(\mathbf{R}_{\mathbf{h}_{i,j}^{0,k}}, \mathbf{R}_{\mathbf{h}_{i,j}^{1,k}}, ..., \mathbf{R}_{\mathbf{h}_{i,j}^{L-1,k}}), \tag{57}$$

where $\mathbf{R}_{\mathbf{h}_{i,j}^{\ell,k}}$ is a symmetric matrix for the ℓth multipath component of the channel at the kth state, $\mathbf{h}_{i,j}^{\ell,k}$, and consists of σ_ℓ^2 weighted elements equal to $\phi(n) = \sigma_\ell^2 J_0(2\pi f_D n T_s)$ for $n = 0, 1, ..., N_s - 1$.[30]

3.2 | Symbol detection for SMBM-OFDM system

Linear system model given in (42) can be expressed alternatively by replacing real channel coefficients with estimated channel coefficients in the channel matrix similar to (34) to form the definition for symbol detection suitable as

$$\mathbf{y}_{i_{eq}} = \hat{\mathbf{H}}_{eq} \mathbf{s}_{eq} + \mathbf{w}_{i_{eq}}, \tag{58}$$

where $\hat{\mathbf{H}}_{eq}$ can be calculated by substituting $\hat{\mathbf{h}}_{i,j}^{\ell,k} = \mathbf{\Psi}_{i,j}^k \hat{\mathbf{c}}_{i,j}^{\ell,k}$) similar to the expression defined in (35) instead of $\mathbf{h}_{i,j}^{\ell,k}$. Since pilot sequence information is available at the receiver, the transmitted signal vector can be broken down into two segments (i.e., pilot and data) as

$$\mathbf{y}_{i_{eq}} = \hat{\mathbf{H}}_{\mathbf{p}} \mathbf{p} + \hat{\mathbf{H}}_{\mathbf{d}} \mathbf{d} + \mathbf{w}_{i_{eq}}, \tag{59}$$

where $\hat{\mathbf{H}}_{\mathbf{p}}$ and $\hat{\mathbf{H}}_{\mathbf{d}}$ denote the column matrices extracted from $\hat{\mathbf{H}}_{eq}$ considering the index locations of pilot and data samples in the transmitted signal, respectively, while $\mathbf{p} = [\mathbf{p}_1, \mathbf{p}_2, ..., \mathbf{p}_{\lambda+1}]^T$ is the utilized composite training sequence vector and $\mathbf{d} = [\mathbf{d}_1, \mathbf{d}_2, ..., \mathbf{d}_\lambda]^T$ is the transmitted OFDM signal vector.

In addition, estimated channel matrix can be defined as a combination of its column vectors as

$$\hat{\mathbf{H}}_{eq} = [\mathbf{v}_0, \mathbf{v}_1, ..., \mathbf{v}_{N_s-1}] \ \in \mathbb{C}^{N_f \times N_s}. \tag{60}$$

Accordingly, the decomposed channel matrices, constructed based on the time indices of pilot sequence and OFDM data in the transmitted signal vector, can be written as

$$\hat{\mathbf{H}}_{\mathbf{p}} = \left[\hat{\mathbf{H}}_{\mathbf{p}_0}, \hat{\mathbf{H}}_{\mathbf{p}_1}, ..., \hat{\mathbf{H}}_{\mathbf{p}_\lambda}\right], \tag{61}$$

$$\hat{\mathbf{H}}_{\mathbf{d}} = \left[\hat{\mathbf{H}}_{\mathbf{d}_1}, \hat{\mathbf{H}}_{\mathbf{d}_2}, ..., \hat{\mathbf{H}}_{\mathbf{d}_\lambda}\right], \tag{62}$$

where $\{\hat{\mathbf{H}}_{\mathbf{p}_q}\}_{q=0}^{\lambda}$ and $\{\hat{\mathbf{H}}_{\mathbf{d}_q}\}_{q=1}^{\lambda}$ are the submatrices extracted from the $\hat{\mathbf{H}}_{eq}$ through its column vectors that correspond to the related indices of pilot and data sequences, respectively.

Then, OFDM data symbols can be estimated as

$$\hat{\mathbf{d}}_i = (\hat{\mathbf{H}}_{\mathbf{d}}^\dagger \hat{\mathbf{H}}_{\mathbf{d}} + N_0 \mathbf{R}_{\mathbf{d}}^{-1})^{-1} \hat{\mathbf{H}}_{\mathbf{d}}^\dagger (\mathbf{y}_i - \hat{\mathbf{H}}_{\mathbf{p}} \mathbf{p}), \tag{63}$$

where $\mathbf{R}_{\mathbf{d}} = \frac{1}{N} \mathbf{I}_N$ denotes the autocorrelation matrix of the OFDM data symbols in time-domain. To find the frequency domain equivalent of estimated symbols, Fourier transform is applied as

$$\hat{\mathbf{b}}_i = \mathbf{F}\hat{\mathbf{d}}_i. \tag{64}$$

Consequently, the decision maker at the receiver operates to decide the symbols according to the selected modulation type regarding ML detection.

4 | SYSTEM PERFORMANCE METRICS

The system performance is evaluated by means of channel estimation error (i.e., MSE) and symbol detection error (i.e., SER). To measure the efficiency and success of the proposed channel estimation method, BCRB which shows the attainable minimum error level for channel estimation is derived theoretically. On the other hand, receiver computational complexity analysis can be determined easily with respect to the number of complex multiplications (CMs) thanks to the implementation simplicity of the LMMSE algorithm.

4.1 | Mean square error definition for channel estimation

Average MSE can be expressed to calculate the channel estimation error and can be determined as

$$\begin{aligned} \mathrm{MSE}_{\mathbf{h}_i} &= \frac{1}{N_s N_t N_{map} L}\mathbb{E}\left[\left(\mathbf{h}_i - \widehat{\tilde{\mathbf{h}}}_i\right)^{\dagger}\left(\mathbf{h}_i - \widehat{\tilde{\mathbf{h}}}_i\right)\right] \\ &= \frac{1}{N_s L}\mathbb{E}\left[\left(\mathbf{h}_{i,j}^{k} - \widehat{\tilde{\mathbf{h}}}_{i,j}^{k}\right)^{\dagger}\left(\mathbf{h}_{i,j}^{k} - \widehat{\tilde{\mathbf{h}}}_{i,j}^{k}\right)\right]. \end{aligned} \tag{65}$$

In addition, BCRB derivation is included in Appendix A and is related with the channel estimation error addressed in (65) as

$$\mathrm{MSE}_{\mathbf{h}_i} \geq \frac{1}{N_s L}\mathrm{trace}\left\{\left(N_0{}^{-1}\boldsymbol{\Gamma}_i^{\dagger}\boldsymbol{\Gamma}_i + 2\boldsymbol{\Sigma}_{\mathbf{c}_{i,j}^{k}}^{-1}\right)^{-1}\right\}, \tag{66}$$

where $\boldsymbol{\Sigma}_{\mathbf{c}_{i,j}^{k}}$ stands for the covariance matrix of channel basis coefficients and can be determined considering the prior probability density function of each channel basis coefficients, $p(\mathbf{c}_{i,j}^{\ell,k})$ that can be defined as $\mathbf{c}_{i,j}^{\ell,k} \sim \mathbb{N}(\mathbf{0}, \boldsymbol{\Sigma}_{\mathbf{c}_{i,j}^{\ell,k}})$. Then, the covariance matrix of channel basis coefficients can be represented as

$$\boldsymbol{\Sigma}_{\mathbf{c}_{i,j}^{k}} = \mathrm{diag}(\boldsymbol{\Sigma}_{\mathbf{c}_{i,j}^{0,k}}, \boldsymbol{\Sigma}_{\mathbf{c}_{i,j}^{1,k}}, ..., \boldsymbol{\Sigma}_{\mathbf{c}_{i,j}^{L-1,k}}), \tag{67}$$

where

$$\boldsymbol{\Sigma}_{\mathbf{c}_{i,j}^{\ell,k}} = \boldsymbol{\Psi}_{i,j}^{k^{\dagger}}\mathbf{R}_{\mathbf{h}_{i,j}^{\ell,k}}\boldsymbol{\Psi}_{i,j}^{k} \in \mathbb{C}^{\lambda\times\lambda}. \tag{68}$$

4.2 | Computational complexity

As the method for estimating both channel and symbols is LMMSE, the computational complexity of this algorithm is directly related with CMs during the calculation. Channel estimation complexity can be calculated by using (55) with D denoting the length of the useful observation vector. The computational complexity can be expressed easily as $\mathbb{O}\left(D(\lambda L)^2\right)$ since the length of the reduced-sized observation signal (i.e., D) is usually bigger than the length of the basis coefficient vector (i.e., λL). It can be inferred that the total computation complexity depends on the ISI-free region

length and basis coefficient length and seen to be relatively low compared to the algorithms that require recursive iterations including SAGE algorithm[38] and Kalman filter methods[39] with higher computational loads, $\mathbb{O}(NL)$ and $\mathbb{O}(N^2)$, respectively.

5 | SIMULATION RESULTS

In this section, we present the performance results of channel estimation and symbol detection of the proposed SMBM-OFDM systems together with the SM-OFDM systems as a benchmark comparison; 4×4 MIMO systems for both systems are considered where $N_t = N_r = 4$. The transmitted OFDM signal comprises $N = 256$ data subcarriers and $N_p = 32$ pilot subcarriers where PN sequences are deployed as pilot subcarriers by selecting $a = 5$ meeting the coprimeness condition defined in (6). The number of RF mirrors at each antenna used to modulate independent channel fade realizations is selected as $N_{RF} = 2$, that is, $2^{N_{RF}} = 4$ channel realizations are available between active transmit antenna and each receive antennas. The multipath number of fast time-varying wireless environments are shown to be limited under highly mobile channel conditions.[30,38] Accordingly, the simulated channel scenario is similar with the environment tested for conventional CP-OFDM systems as defined in Senol et al[38] and Basaran et al[40] under same conditions in terms of channel multipath number. Channel multipath number is chosen as $L = 3$ where the channel coefficients are modeled by WSSUS Rayleigh distribution with normalized path powers determined as $\sigma_0^2 = 0.448, \sigma_1^2 = 0.321$, and $\sigma_2^2 = 0.230$. Note that the simulated scenario can be easily applied to the channel environments with more than three multipath components by suitably adjusting PN sequence lengths to allow the occurrence of ISI-free regions in order to make channel estimation possible. The normalized Doppler frequencies due to the fast time-varying channel environment are specified as $f_D T = \{0.04, 0.08\}$ results in mobile speeds of $\nu = \{240, 480\}$ km/h, respectively, where corresponding number of basis coefficients are $\lambda = \{2, 3\}$, respectively, considering the BEM approximation error around 10^{-6}.[38] Multiple pilot sequences are deployed with lengths $N_{p_1} = N_{p_2} = 11, N_{p_3} = 10$ when $\lambda = 2$ and $N_{p_i} = 8$ for $i = 1, 2, 3, 4$ when $\lambda = 3$ while the corresponding OFDM data lengths $N_i = 128$ for $i = 1, 2$ when $\lambda = 2$ and $N_1 = N_2 = 85, N_3 = 86$ when $\lambda = 3$, respectively. As per the symbol detection evaluation, using the estimation of data symbols in frequency domain defined in (64), the detected modulated symbols can be determined by the application of ML rule regarding the selected modulation type. Indicating the detected symbols by $\tilde{\mathbf{b}}_i$, the SER at each antenna can be calculated as the ratio of the total number of the erroneously detected symbols to the length of the transmit signal. Accordingly, BPSK, QPSK, and 16-QAM modulation types are operated for demonstrating symbol detection performance.

In Figure 3, channel estimation performance of SM-OFDM and SMBM-OFDM systems are shown for the normalized Doppler frequencies $f_D T = \{0.04, 0.08\}$ that correspond to $\lambda = \{2, 3\}$ and $\nu = \{240, 480\}$ km/h, respectively, when BPSK modulation is selected. Corresponding achievable error bounds, BCRBs, are also included. It is observed that the

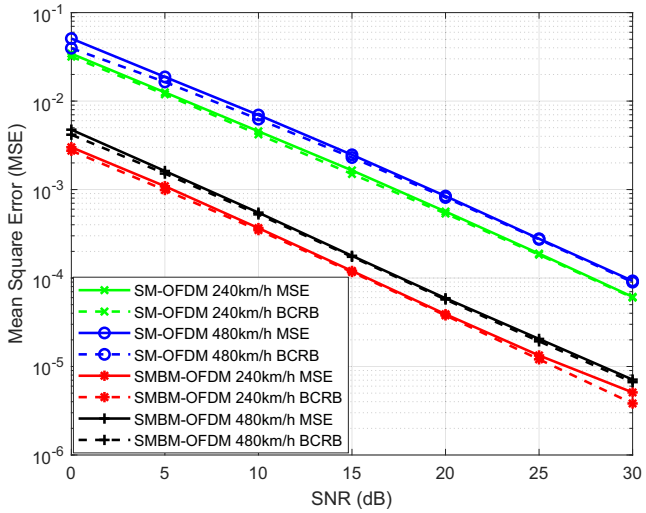

FIGURE 3 Channel estimation error performances of 4×4 SM-OFDM and 4×4 SMBM-OFDM systems

estimation performance of MBM applied system outperforms conventional SM-OFDM system under the same conditions demonstrating the superiority of the MBM concept. For instance, 4×4 MIMO SMBM-OFDM system has around 12 dB SNR gain compared to conventional SM-OFDM system since it naturally utilizes channel modifications due to the implementation of MBM considering the channel reconstruction error level fixed at 10^{-4}. Moreover, channel estimation performance at lower mobile speeds (with $\lambda = 2$) is better than the performance at higher mobile speeds (with $\lambda = 3$) since orthogonality among subcarriers in OFDM is corrupted under high mobility. Furthermore, LMMSE-based channel estimation performances are nearly the perfect since BCRB levels are attained almost each SNR values demonstrating that the proposed channel estimation approach is suitable for fast time-varying channel environments.

In Figure 4, the detection performance of conventional 4×4 SM-OFDM and 4×4 SMBM-OFDM systems is presented when BPSK modulation is adopted for the same parameters. Similar to the interpretation on channel estimation performance, SER of MBM applied OFDM system is better compared to conventional SM-OFDM system. On the other hand, an increase in the mobile speed (i.e., Doppler spread) results in enhanced symbol detection performance since a shift in Doppler frequency permits receiver to make use of time diversity better in contrast to the channel estimation results.

In Figure 5, SER performances are illustrated under same conditions for QPSK modulated systems. Due to the increase in modulation level, the corresponding symbol detection performance gets worse compared to BPSK case. In

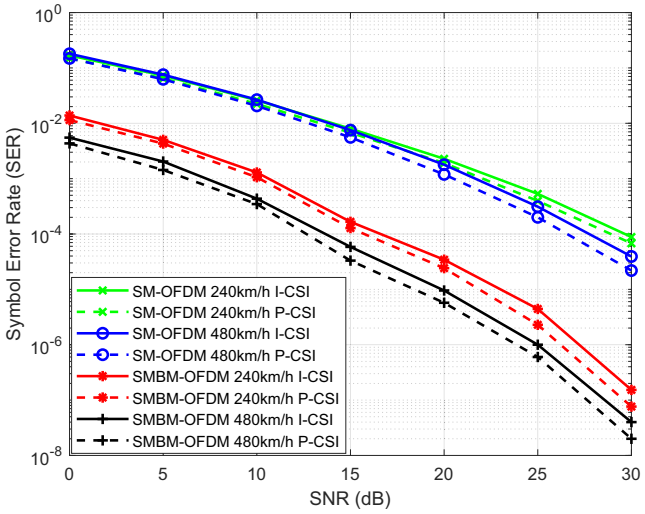

FIGURE 4 BPSK modulated symbol detection error performances of 4×4 SM-OFDM and 4×4 SMBM-OFDM systems

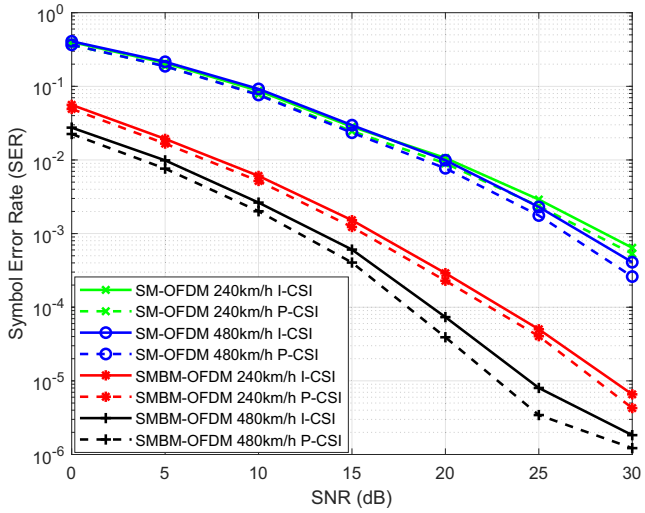

FIGURE 5 QPSK modulated symbol detection error performances of 4×4 SM-OFDM and 4×4 SMBM-OFDM systems

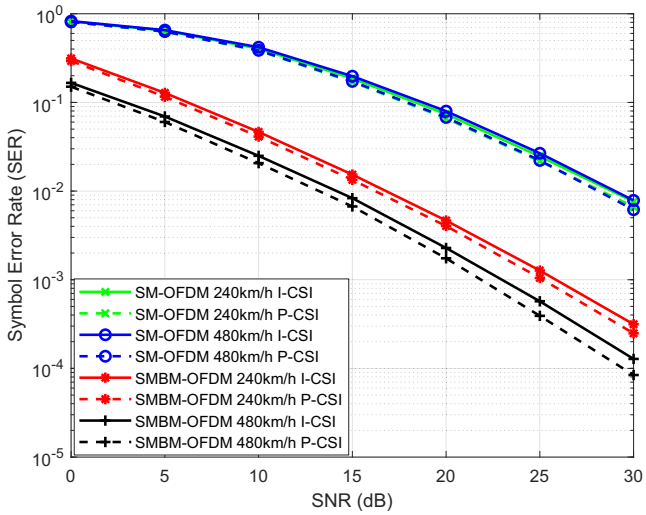

FIGURE 6 16-QAM modulated symbol detection error performances of 4 × 4 SM-OFDM and 4 × 4 SMBM-OFDM systems

addition, detection performance results of QPSK modulated systems decrease approximately 10 times in terms of SER compared to BPSK modulated systems.

Finally, 16-QAM modulated SM-OFDM and SMBM-OFDM system performance are presented in Figure 6 where SER values decrease due to elimination of time diversity stemming from the modulation level compared to the results belonging to QPSK modulated systems. Note that 16-QAM SER performance of SM-OFDM system behavior at lower mobile speeds are almost same to that of higher speeds on the contrary to SMBM-OFDM system. This stems from the lack of time diversity advantage in conventional OFDM system receivers which can be provided by SM-MBM integration. In other words, SMBM-OFDM system is able to provide both rich time diversity and better SER results even in higher order modulations and high mobility.

6 | CONCLUSION

In this paper, SMBM-OFDM system has been proposed as a new modulation technique that can be a potential for next generation wireless communications. In addition, a new channel estimation perspective for MBM-based systems under high mobility has been proposed under fast time-varying channel environment for the first time with improved system performance. Time-varying channel conditions in MBM have been modeled by BEM to reduce the number of unknown channel coefficients, and therefore, make channel estimation possible. It has been revealed that the LMMSE-based channel estimation performance with PN sequence deployment is able to well approach to the derived theoretical lower bound, BCRB thanks to its optimality. It has been also shown that the channel estimation and symbol detection performance of MBM applied system is superior to the conventional SM-OFDM systems. In addition, the symbol detection performance of the proposed SMBM-OFDM systems provides significantly better results (i.e., around 12-dB performance gains) even in highly mobile environments. As the channel estimation is quite challenging in MBM due to the modulation in medium, the results of this study are quite important for demonstrating the realistic channel estimation performance of the proposed SMBM-OFDM systems under highly mobile wireless communications.

DATA AVAILABILITY STATEMENT

Data sharing is not applicable to this article as no datasets were generated or analyzed during the current study.

ORCID

Mehmet Başaran https://orcid.org/0000-0002-5473-1437
Ertuğrul Başar https://orcid.org/0000-0001-5566-2392
Hakan Ali Çırpan https://orcid.org/0000-0002-3591-6567

REFERENCES

1. Vitturi S, Zunino C, Sauter T. Industrial communication systems and their future challenges: next-generation ethernet, IIoT, and 5G. *Proc IEEE*. 2019;107(6):944-961. doi:10.1109/JPROC.2019.2913443
2. Siddiqi MA, Yu H, Joung J. 5G ultra-reliable low-latency communication implementation challenges and operational issues with IoT devices. *Electronics*. 2019;8(9):1-18.
3. 3GPP. Technical Specification Group Services and System Aspects. Technical Specification (TS) 21.915, 3rd Generation Partnership Project (3GPP); Version 15.0.0; 2019.
4. Basar E, Wen M, Mesleh R, Di Renzo M, Xiao Y, Haas H. Index modulation techniques for next-generation wireless networks. *IEEE Access*. 2017;5:16693-16746. doi:10.1109/ACCESS.2017.2737528
5. Hamamreh JM, Basar E, Arslan H. OFDM-subcarrier index selection for enhancing security and reliability of 5G URLLC services. *IEEE Access*. 2017;5:25863-25875.
6. Larsson EG, Edfors O, Tufvesson F, Marzetta TL. Massive MIMO for next generation wireless systems. *IEEE Commun Mag*. 2014;52(2):186-195. doi:10.1109/MCOM.2014.6736761
7. Basar E. Index modulation techniques for 5G wireless networks. *IEEE Commun Mag*. 2016;54(7):168-175. doi:10.1109/MCOM.2016.7509396
8. Tusha A, Dogan S, Arslan H. A hybrid downlink NOMA with OFDM and OFDM-IM for beyond 5G wireless networks. *IEEE Signal Process Lett*. 2020;27:491-495.
9. Wen M, Zheng B, Kim KJ, et al. A survey on spatial modulation in emerging wireless systems: research progresses and applications. *IEEE J Sel Areas Commun*. 2019;37(9):1949-1972.
10. Serafimovski N, Younis A, Mesleh R, et al. Practical implementation of spatial modulation. *IEEE Trans Veh Technol*. 2013;62(9):4511-4523. doi:10.1109/TVT.2013.2266619
11. Ganesan S, Mesleh R, Ho H, Ahn CW, Yun S. On the performance of spatial modulation OFDM. In: Fortieth Asilomar Conf. Signals, Syst. and Computers; 2006:1825-1829.
12. Khandani AK. Media-based modulation: converting static Rayleigh fading to AWGN. In: IEEE Int. Symp. Inf. Theory; 2014:1549-1553.
13. Khandani AK. Media-based modulation: a new approach to wireless transmission. In: IEEE Int. Symp. Inf. Theory; 2013:3050-3054.
14. Shamasundar B, Chockalingam A. Multiuser media-based modulation for massive MIMO systems. In: IEEE 18th Int. Workshop Signal Process. Advances in Wireless Commun. (SPAWC); 2017:1-5.
15. Yildirim I, Basar E, Altunbas I. Quadrature channel modulation. *IEEE Wireless Commun Lett*. 2017;6(6):790-793. doi:10.1109/LWC.2017.2742508
16. Bamisaye AJ, Quazi T. Quadrature spatial modulation-aided single-input multiple-output-media-based modulation. *Int J Commun Syst*. 2021;34(11):e4883. doi:10.1002/dac.4883
17. Basar E, Altunbas I. Space-time channel modulation. *IEEE Trans Veh Technol*. 2017;66(8):7609-7614. doi:10.1109/TVT.2017.2674689
18. Yigit Z, Basar E. Space-time media-based modulation. *IEEE Trans Signal Process*. 2019;67(9):2389-2398. doi:10.1109/TSP.2019.2905836
19. Naresh Y, Chockalingam A. On media-based modulation using RF mirrors. *IEEE Trans Veh Technol*. 2017;66(6):4967-4983. doi:10.1109/TVT.2016.2620989
20. Oladoyinbo S, Pillay N, Xu H. Media-based single-symbol generalized spatial modulation. *Int J Commun Syst*. 2019;32(6):e3909. IJCS-18-0541.R1. doi:10.1002/dac.3909
21. Naresh Y, Chockalingam A. Performance analysis of media-based modulation with imperfect channel state information. *IEEE Trans Veh Technol*. 2018;67(5):4192-4207. doi:10.1109/TVT.2018.2791845
22. Shamasundar B, Jacob S, Theagarajan LN, Chockalingam A. Media-based modulation for the uplink in massive MIMO systems. *IEEE Trans Veh Technol*. 2018;67(9):8169-8183. doi:10.1109/TVT.2018.2839706
23. Naresh Y, Chockalingam A. A low-complexity maximum-likelihood detector for differential media-based modulation. *IEEE Commun Lett*. 2017;21(10):2158-2161. doi:10.1109/LCOMM.2017.2687921
24. Ma Q, Yang P, Xiao Y, Bai H, Li S. Error probability analysis of OFDM-IM with carrier frequency offset. *IEEE Commun Lett*. 2016;20(12):2434-2437. doi:10.1109/LCOMM.2016.2600646
25. Kabaci A, Basaran M, Cirpan HA. Reference signal-aided channel estimation in spatial Media-Based modulation systems. *Physical Commun*. 2020;47:1-7. doi:10.1016/j.phycom.2021.101396
26. Fu Y, Wang C, Ghazal A, Aggoune e M, Alwakeel MM. Performance investigation of spatial modulation systems under non-stationary wideband high-speed train channel models. *IEEE Trans Wireless Commun*. 2016;15(9):6163-6174. doi:10.1109/TWC.2016.2580506
27. Yang P, Xiao Y, Guan YL, Di Renzo M, Li S, Hanzo L. Multidomain index modulation for vehicular and railway communications: a survey of novel techniques. *IEEE Veh Technol Mag*. 2018;13(3):124-134. doi:10.1109/MVT.2018.2814023
28. Acar Y, Aldirmaz-Colak S, Basar E. Channel estimation for OFDM-IM systems. *Turkish J Elec Eng Comp Sci*. 2019;27:1908-1921.
29. Basaran M, Erkucuk S, Senol H, Cirpan HA. Effect of inter-block-interference-free region on compressed sensing based channel estimation in TDS-OFDM systems. In: IEEE Int. Black Sea Conf. on Commun. and Netw. (BlackSeaCom); 2016:1-3.
30. Basaran M, Senol H, Erkucuk S, Cirpan HA. Channel estimation for TDS-OFDM systems in rapidly time-varying mobile channels. *IEEE Trans Wireless Commun*. 2018;17(12):8123-8135. doi:10.1109/TWC.2018.2874228

31. Qasem ZAH, Leftah HA, Sun H, Qi J, Esmaiel H. X-transform time-domain synchronous IM-OFDM-SS for underwater acoustic communication. *IEEE Syst J*. 2021:1-12. doi:10.1109/JSYST.2021.3052470
32. Qasem ZAH, Wang J, Kuai X, Sun H, Esmaiel H. Enabling unique word OFDM for underwater acoustic communication. *IEEE Wireless Commun Lett*. 2021;10(9):1886-1889. doi:10.1109/LWC.2021.3085020
33. Ge X, Yang B, Ye J, Mao G, Wang CX, Han T. Spatial spectrum and energy efficiency of random cellular networks. *IEEE Trans Spatial Commun*. 2015;63(3):1019-1030. doi:10.1109/TCOMM.2015.2394386
34. Zhong Y, Quek TQS, Ge X. Heterogeneous cellular networks with spatio-temporal traffic: delay analysis and scheduling. *IEEE J Sel Areas in Commun*. 2017;35(6):1373-1386. doi:10.1109/JSAC.2017.2687379
35. Ozyurt AB, Basaran M, Ardanuc M, Durak-Ata L, Yanikomeroglu H. Intracell frequency band exiling for green wireless networks: implementation, performance metrics, and use cases. *IEEE Veh Technol Mag*. 2021;16(2):31-39. doi:10.1109/MVT.2021.3057355
36. Chu D. Polyphase codes with good periodic correlation properties (Corresp.) *IEEE Trans Inf Theory*. 1972;18(4):531-532. doi:10.1109/TIT.1972.1054840
37. Jeon WG, Chang KH, Cho YS. An equalization technique for orthogonal frequency-division multiplexing systems in time-variant multipath channels. *IEEE Trans Commun*. 1999;47(1):27-32. doi:10.1109/26.747810
38. Senol H, Panayirci E, Poor HV. Nondata-aided joint channel estimation and equalization for OFDM systems in very rapidly varying mobile channels. *IEEE Trans Signal Process*. 2012;60(8):4236-4253. doi:10.1109/TSP.2012.2195657
39. Hijazi H, Ros L. Joint data QR-detection and Kalman estimation for OFDM time-varying Rayleigh channel complex gains. *IEEE Trans Commun*. 2010;58(1):170-178. doi:10.1109/TCOMM.2010.01.080296
40. Basaran M, Macit MC, Senol H, Erkucuk S. Realistic channel estimation of IEEE 802.11af systems in TV white space. *IEEE Trans Veh Technol*. 2020;69(10):11066-11076. doi:10.1109/TVT.2020.3007341

How to cite this article: Başaran M, Başar E, Çırpan HA. High mobility enabled spatial and media-based modulated orthogonal frequency division multiplexing systems for beyond 5G wireless communications. *Int J Commun Syst*. 2022;35(8):e5114. doi:10.1002/dac.5114

APPENDIX A

[BCRB Derivation] Considering the Bayesian estimator defined in Basaran et al[30] for (46), the covariance matrix of channel basis coefficients error can be written as

$$\mathbb{E}_{\mathbf{z}_i,\mathbf{c}_{i,j}^k}\left[(\hat{\mathbf{c}}_{i,j}^k-\mathbf{c}_{i,j}^k)(\hat{\mathbf{c}}_{i,j}^k-\mathbf{c}_{i,j}^k)^{\dagger}\right]\geq(\mathbf{J}+\boldsymbol{\Sigma}_{\mathbf{c}_{i,j}^k}^{-1})^{-1}, \tag{A1}$$

where $\mathbf{J}$ and $\boldsymbol{\Sigma}_{\mathbf{c}_{i,j}^k}$ denote the Bayesian Fisher information matrix (BFIM) and the error covariance matrix of channel basis coefficients, respectively. BFIM can be expressed as

$$\begin{aligned}\mathbf{J} &= \mathbf{J}_d+\mathbf{J}_p\\ &\triangleq -\mathbb{E}_{\mathbf{z}_i,\mathbf{c}_{i,j}^k}\left[\frac{\partial^2\log p(\mathbf{z}_i|\mathbf{c}_{i,j}^k)}{\partial\mathbf{c}_{i,j}^{k\,*}\,\partial\mathbf{c}_{i,j}^{k\,T}}\right]-\mathbb{E}_{\mathbf{z}_i,\mathbf{c}_{i,j}^k}\left[\frac{\partial^2\log p(\mathbf{c}_{i,j}^k)}{\partial\mathbf{c}_{i,j}^{k\,*}\,\partial\mathbf{c}_{i,j}^{k\,T}}\right],\end{aligned} \tag{A2}$$

considering the equality $p(\mathbf{z}_i,\mathbf{c}_{i,j}^k)=p(\mathbf{z}_i|\mathbf{c}_{i,j}^k)p(\mathbf{c}_{i,j}^k)$, where the first and second terms in the summation above (i.e., $\mathbf{J}_d$ and $\mathbf{J}_p$) can be called data FIM (DFIM) and prior FIM (PFIM), respectively. DFIM can be further distinguished as

$$\mathbf{J}_d=-\mathbb{E}_{\mathbf{z}_i|\mathbf{c}_{i,j}^k}\left[\frac{\partial^2\log p(\mathbf{z}_i|\mathbf{c}_{i,j}^k)}{\partial\mathbf{c}_{i,j}^{k\,*}\,\partial\mathbf{c}_{i,j}^{k\,T}}\right]. \tag{A3}$$

Since $\mathbf{c}_{i,j}^k\sim\mathbb{CN}(\mathbf{0},\boldsymbol{\Sigma}_{\mathbf{c}_{i,j}^k})$, $p(\mathbf{z}_i|\mathbf{c}_{i,j}^k)$ can be represented utilizing the complex Gaussian distribution property as

$$p(\mathbf{z}_i|\mathbf{c}_{i,j}^k) = \frac{1}{(\Pi N_0)^D}\exp\left(-{N_0}^{-1}(\mathbf{z}_i - \boldsymbol{\Gamma}_i\mathbf{c}_{i,j}^k)^{\dagger(\mathbf{z}_i-\boldsymbol{\Gamma}_i\mathbf{c}_{i,j}^k)}\right). \tag{A4}$$

After simple mathematical operations, DFIM can be determined as

$$\mathbf{J}_d = {N_0}^{-1}\boldsymbol{\Gamma}_i^{\dagger}\boldsymbol{\Gamma}_i. \tag{A5}$$

The prior information distribution of channel basis coefficients can be written as

$$p(\mathbf{c}_{i,j}^k) = \frac{1}{\Pi^{\lambda L}\det|\boldsymbol{\Sigma}_{\mathbf{c}_{i,j}^k}|}\exp\left(-\mathbf{c}_{i,j}^{k\,\dagger}\boldsymbol{\Sigma}_{\mathbf{c}_{i,j}^k}^{-1}\mathbf{c}_{i,j}^k\right). \tag{A6}$$

Therefore, regarding the above definition, PFIM, can be obtained as

$$\mathbf{J}_p = \boldsymbol{\Sigma}_{\mathbf{c}_{i,j}^k}^{-1}. \tag{A7}$$

Then, using the related equations (A2), (A5), and (A7), covariance matrix of channel basis coefficient estimation defined in (A1) can be rewritten as

$$\mathbb{E}_{\mathbf{z}_i,\mathbf{c}_{i,j}^k}\left[(\hat{\mathbf{c}}_{i,j}^k - \mathbf{c}_{i,j}^k)(\hat{\mathbf{c}}_{i,j}^k - \mathbf{c}_{i,j}^k)^{\dagger}\right] \geq \left({N_0}^{-1}\boldsymbol{\Gamma}_i^{\dagger}\boldsymbol{\Gamma}_i + 2\boldsymbol{\Sigma}_{\mathbf{c}_{i,j}^k}^{-1}\right)^{-1}. \tag{A8}$$

The average MSE of channel basis coefficients follow the summation of the diagonal components of the inverse matrix defined in (A8), and thus, the relationship between BCRB and the average MSE of basis coefficients can be represented as

$$\begin{aligned}\mathrm{MSE}_{\mathbf{c}_i} &= \frac{1}{\lambda L}\sum_{\ell}\mathbb{E}\left[(\mathbf{c}_{i,j}^{\ell,k} - \hat{\mathbf{c}}_{i,j}^{\ell,k})^{\dagger}(\mathbf{c}_{i,j}^{\ell,k} - \hat{\mathbf{c}}_{i,j}^{\ell,k})\right] \\ &\geq \mathrm{trace}\left\{\left({N_0}^{-1}\boldsymbol{\Gamma}_i^{\dagger}\boldsymbol{\Gamma}_i + 2\boldsymbol{\Sigma}_{\mathbf{c}_{i,j}^k}^{-1}\right)^{-1}\right\}.\end{aligned} \tag{A9}$$

Recall that the average MSE of channel coefficient definition provided below

$$\mathrm{MSE}_{\mathbf{h}_i} = \frac{1}{N_s L}\mathbb{E}\left[\left(\mathbf{h}_{i,j}^k - \widehat{\widetilde{\mathbf{h}}}_{i,j}^k\right)^{\dagger}\left(\mathbf{h}_{i,j}^k - \widehat{\widetilde{\mathbf{h}}}_{i,j}^k\right)\right] \tag{A10}$$

can be represented in terms of BEM transformation (i.e., $\widehat{\widetilde{\mathbf{h}}}_{i,j}^k = \boldsymbol{\Phi}_{i,j}^k\hat{\mathbf{c}}_{i,j}^k$), as

$$\mathrm{MSE}_{\mathbf{h}_i} = \frac{1}{N_s L}\sum_{\ell}\mathbb{E}\left[(\mathbf{c}_{i,j}^{\ell,k} - \hat{\mathbf{c}}_{i,j}^{\ell,k})^{\dagger}(\mathbf{c}_{i,j}^{\ell,k} - \hat{\mathbf{c}}_{i,j}^{\ell,k})\right] = \frac{\lambda}{N_s}\mathrm{MSE}_{\mathbf{c}_i} \tag{A11}$$

since $\boldsymbol{\Phi}_{i,j}^{k^{\dagger}}\boldsymbol{\Phi}_{i,j}^k = \mathbf{I}_{\lambda L}$.

Finally, BCRB derivation can be represented in closed form as

$$\mathrm{MSE}_{\mathbf{h}_i} \geq \frac{1}{N_s L}\mathrm{trace}\left\{\left({N_0}^{-1}\boldsymbol{\Gamma}_i^{\dagger}\boldsymbol{\Gamma}_i + 2\boldsymbol{\Sigma}_{\mathbf{c}_{i,j}^k}^{-1}\right)^{-1}\right\}. \tag{A12}$$